Influence of the North Atlantic on simulated atmospheric variability

Sébastien Conil and Zhao X. Li
Laboratoire de Météorologie Dynamique, CNRS, Université Pierre et Marie Curie, Paris, France

Abstract
An atmospheric general circulation model is used to investigate the influence of the North Atlantic Ocean on atmospheric variability. The study covers the period from 1950 to 1994. The observed sea surface temperature and sea ice extension are used to force the atmospheric model. Several configurations of the oceanic boundary conditions were made to isolate the role of the North Atlantic and to study its non-linear interaction with forcings from other oceanic basins. The multi-realization character of the experiments distinguishes between the internal random part and the external forced part of the total variability. The potential predictability can thus be evaluated. The response of the atmosphere is also studied with a modal approach in terms of hemispheric teleconnection patterns. The North Atlantic Ocean has a direct influence on both the Northern Hemisphere annular mode and the Pacific-North-America pattern, leading to a weak predictability. However the direct response is largely modulated by forcings from other oceanic basins. The non-linearity of the system compensates the predictable component of the annular mode induced by the North Atlantic forcing. Furthermore it reduces the forced component of the Pacific-North-America pattern, increasing its chaoticity.

Key words *atmospheric general circulation model – internal/external variability – climate predictability – teleconnections*

1. Introduction

Atmospheric circulation of the Northern Hemisphere exhibits variability in a wide range of timescales, from days to decades (see Feldstein, 2000). This variability is dominated by a small number of large-scale coherent teleconnection patterns (Wallace and Gutzler, 1981), such as the PNA (Pacific-North-America pattern) or the NAO (North Atlantic Oscillation). They have major climatic impacts and are involved in many climate phenomena. Understanding the mechanisms controlling the teleconnection patterns will contribute to make reliable climate predictions at different time scales.

Predictability of the climate at seasonal to decadal timescales arises from two distinct sources as described by Lorenz (1975). The first source is the initial states (initial-value problem) and the second one is the boundary conditions (potential predictability). They are called the first and second kinds of predictability respectively (Collins and Allen, 2002). When an atmospheric general circulation model is used to investigate the second kind of predictability, the boundary conditions are the SST and sea-ice variation. A number of past studies looking for the role of the ocean in building atmospheric variability and its associated predictability utilize forced AGCM, as in Harzallah and Sadourny (1995) and Zwiers *et al.* (2000). They note a robust high predictability in the low latitudes whereas the extra-tropical regions show weak (and inconsistent) response.

Mailing address: Dr. Sébastien Conil, Laboratoire de Météorologie Dynamique, CNRS, Université Pierre et Marie Curie, casier 99, 4 place Jussieu,75252 Paris Cedex 05, France; e-mail: conil@lmd.jussieu.fr

Tropical oceanic forcing has been used with success, in the TOGA (Tropical Ocean-Global Atmosphere) context, to understand ENSO-related (El Niño Southern Oscillation) teleconnections and to forecast associated climate fluctuations (Trenberth *et al.*, 1998). The role of the mid-latitude ocean is however much more controversial (see Kushnir *et al.*, 2002). In particular, the role of the North Atlantic for low-frequency climate variability is very uncertain. Results reported in the literature are often incoherent. Rodwell *et al.* (1999) reported a high hindcast skill of the NAO, originated from the North Atlantic decadal- scale variation by using an atmospheric general circulation model forced by the observed SST for the second half of the 20th century. Similar experiments were also repeated by other groups, Latif *et al.* (2000), for example, pointed out that a considerable part of this hindcast skill came from the Equatorial Pacific through global teleconnection mechanisms. The ENSO influence on the North Atlantic and Europe atmospheric variability was also depicted in Fraedrich (1994) or Venzke *et al.* (1999).

Lack of a suitable theoretical framework is the main obstacle to understand the role of the mid-latitude ocean in forcing climate variability. In fact, mid-latitude atmospheric circulation is characterized by a strong transient circulation with large-scale wave-like structures. Response of such a regime of atmospheric circulation to the boundary conditions is much more complex. Strong scale-interactions also increase the difficulties in understanding the role of the mid-latitude ocean. For the synoptic time scales, mid-latitude ocean has mainly a passive role in integrating the atmospheric variation, such as surface temperature or wind stress. The ocean-to-atmosphere signal at low-frequency scale is often masked by the high-frequency atmosphere-to-ocean patterns (Frankignoul, 1985).

In this work we address the problem of the influence of the oceanic boundary conditions on atmospheric variability in the Northern Hemisphere. This work is a natural extension of Li (1999) with emphasis on the role of the North Atlantic Ocean. We will study the atmospheric response to the oceanic boundary conditions, by separating internal from external variability. Our aim is also to identify the teleconnection structures that are sensitive to the oceanic forcing. We will particularly focus on the influence of the North Atlantic and its possible interaction with forcing from other oceanic basins.

Three configurations corresponding to different oceanic boundary conditions are used. The first experiment uses the global observed oceanic surface conditions. To emphasize the North Atlantic role, we perform two other experiments, one forced by observed varying oceanic conditions only in the North Atlantic and climatological conditions elsewhere, the other with climatological oceanic conditions in the North Atlantic and observed varying forcing elsewhere. Such a strategy allows us to assess the influence of the North Atlantic Ocean in two complementary ways. In fact the North Atlantic ocean can have a direct impact on the atmospheric variability, but its influence can be non linear and the direct impact can be modulated by other oceanic forcing. This non-linearity can also act on the internal variability.

The structure of the paper is as follows. Model, experimental design and statistical methods are briefly described in Section 2. Results on the simulated variability, its internal and external decompositions, and the potential predictability are presented in Section 3. In Section 4 we focus on the spatial modes of variability and their predictability. Discussion and conclusion are given in Section 5.

2. Model, experiments and analysis method

2.1. *Model description*

The model used in this study is LMDZ version 3.3, a state-of-the-art climate model derived from the standard version, as described in Sadourny and Laval (1984). The model is formulated through finite-difference on the Arakawa-C grid. Its horizontal resolution is 4° in latitude and 5° in longitude, with regularly distributed grid points. The model uses vertical hybrid coordinates with 19 levels, unevenly spaced to allow a better resolution in the boundary layer. The advection scheme is designed to conserve potential enstrophy for divergent barotropic flow (Sadourny, 1975). Lateral diffu-

sion is calculated through an iterated Laplacian operator. Six minutes are the time step used to resolve the dynamics, but the physical parameterizations are evaluated only every 30 min. Convection is parameterized with a simple mass-flux scheme developed by Tiedtke (1989). The cloud parameterization, presented in Le Treut and Li (1991), uses a cloud water budget and a statistical description of the subgrid water distribution. The radiation package is the same as that used in the model of ECMWF. The short-wave radiation code is an updated version of the Fouquart and Bonnel (1980) scheme. Long-wave radiation scheme was designed by Morcrette (1991). The planetary boundary layer scheme is based on a second order closure model. The surface model is a bucket model for which we consider a homogeneous layer of 150 mm. Calculation of the surface temperature is incorporated in the boundary layer and based on the surface energy balance equation. For the surface moisture, a holding capacity is fixed at 150 mm of water, and all the water above this value is lost as runoff. A complete description of the model is available at «http://www.lmd.jussieu.fr/~lmdz/doc.html». The same version of the GCM was also used in the coupled ocean - atmosphere study presented in Li and Conil (2003).

2.2. *Realization of experiments*

Our main objective is to study the influence of the North Atlantic oceanic conditions on atmospheric variability and predictability. The separation of external and internal components of the total variability and the evaluation of the potential predictability require an ensemble approach. The ensemble size is critical because the signal-to-noise ratio is weak as shown by Li (1999) and Mehta *et al.* (2000). We adopt thus the ensemble approach for all the three experiments.

An ensemble of 17 simulations was first run with global SST and sea-ice distributions as boundary conditions, covering the period 1950-1994. The initial condition differed slightly from one simulation to another. The time-varying SST and sea-ice distributions were obtained from the GISST data set (Rayner *et al.*, 1996), monthly-mean GISST data being interpolated into daily values through a simple spline interpolation scheme. This experiment will be referred to as GLOBAL. In order to isolate the role of the North Atlantic oceanic boundary conditions two additional experiments (referred to as NOATL and ATL, hereafter) were also performed. NOATL consists of 9 integrations with the same SST and sea-ice information for the global ocean, except for the North Atlantic (north of 14°N) where seasonal climatological conditions were prescribed. ATL is a complementary experiment containing also 9 integrations with observed varying SST and sea ice for the North Atlantic Ocean (north of 14°N) but prescribed climatological conditions elsewhere. An additional 150-year integration (referred to as CLIM) was performed with climatological SST and sea ice during the whole integration.

2.3. *Analysis method*

In order to identify the relative influence of the boundary conditions and the internal dynamics in the atmospheric variability, we employed the ANOVA (ANalysis Of VAriance) technique to analyze our ensemble simulations. This approach has been widely used in the past and is described in detail in Harzallah and Sadourny (1995), Rowell (1998) or Von Storch and Zwiers (1999).

If x_i (t, s) represents a variable (*e.g.* winter seasonal-mean geopotential height at 500 hPa) at time t (length $T = 44$ winters) and spatial position s (Northern Hemisphere), for the simulation i (total number $I = 17$ or 9), it can be split into two parts

$$x_i\,(t, s) = E(t, s) + R_i\,(t, s) \qquad (2.1)$$

where E represents the variations induced by varying boundary conditions and R_i the internally-generated variations (the random part). To be able to make this partition, two conditions are necessary (Scheffe, 1959). The first is that E and R follow independent Gaussian distributions, and the second is that E and R are independent. These two conditions are generally verified for variables such as geopotential height or temperature at 500 hPa, since their persistence time scales are much shorter than the year.

Two averages can be defined

$$x_{\mathrm{EM}}(t,s) = \frac{1}{I}\sum_{i=1}^{I} x_i(t,s) \tag{2.2}$$

which is the ensemble mean and

$$\mu(s) = \frac{1}{T}\sum_{t=1}^{T} x_{\mathrm{EM}}(t,s) = \frac{1}{T}\frac{1}{I}\sum_{t=1}^{T}\sum_{i=1}^{I} x_i(t,s) \tag{2.3}$$

which is the general mean or climatological mean.

The ensemble mean is a natural estimator of the boundary-conditions induced variations E, whereas $x_i - x_{\mathrm{EM}}$ is an estimator of the internal variations R_i. The dispersion among the ensemble members gives an unbiased estimate of the internal variability σ_{INT}

$$\sigma^2_{\mathrm{INT}}(s) = \frac{1}{T(I-1)}\sum_{t=1}^{T}\sum_{i=1}^{I}\left(x_i(t,s) - x_{\mathrm{EM}}(t,s)\right)^2. \tag{2.4}$$

The variance σ^2_{EM} of the ensemble mean is given by

$$\sigma^2_{\mathrm{EM}}(s) = \frac{1}{T(I-1)}\sum_{t=1}^{T}\left(x_{\mathrm{EM}}(t,s) - \mu(s)\right)^2. \tag{2.5}$$

Following Scheffe (1959), the oceanic-forced variability σ_{SST} can be deduced from the variance of the ensemble mean after removing the bias due the internal variability

$$\sigma^2_{\mathrm{SST}} = \sigma^2_{\mathrm{EM}} - \frac{1}{I}\sigma^2_{\mathrm{INT}}. \tag{2.6}$$

An unbiased estimate of the total variance σ^2_{TOT} is the sum of the internal and external contributions

$$\sigma^2_{\mathrm{TOT}} = \sigma^2_{\mathrm{SST}} + \sigma^2_{\mathrm{INT}} = \sigma^2_{\mathrm{EM}} + \frac{I-1}{I}\sigma^2_{\mathrm{INT}}. \tag{2.7}$$

In the following, we use the term internal and external variability in reference to σ_{INT} and σ_{SST}. The proportion of the total variance due to the boundary forcing measures the potential predictability

$$\rho = \frac{\sigma^2_{\mathrm{SST}}}{\sigma^2_{\mathrm{TOT}}} = \frac{\sigma^2_{\mathrm{EM}} - \frac{1}{I}\sigma^2_{\mathrm{INT}}}{\sigma^2_{\mathrm{EM}} + \frac{I-1}{I}\sigma^2_{\mathrm{INT}}} = \frac{1}{1 + \frac{I}{\left(I\frac{\sigma^2_{\mathrm{EM}}}{\sigma^2_{\mathrm{INT}}} - 1\right)}}. \tag{2.8}$$

The statistical significance is conducted through a test as in Rowell (1998). The null hypothesis $\sigma^2_{\mathrm{SST}} = 0$ or $\rho = 0$ is rejected at β significance level when

$$\rho > \frac{1}{1 + \frac{I}{F_{T-1;T(I-1);\beta^{-1}}}} \tag{2.9}$$

where $F_{T-1;\,T(I-1);\,\beta}$ is the F statistic at β significance level with degrees of freedom $T-1$ and $T(I-1)$.

3. Analysis of variance and potential predictability

In the following sections we apply the above-described ANOVA technique to the three ensemble experiments, GLOBAL, NOATL and ATL. We focus on the Northern Hemisphere winter, December-January-February, when the variability is stronger, the teleconnections more robust and the potential predictability higher. As mentioned before, the role of the North Atlantic is our particular interest and it can be assessed through combination of the three different experiments. Two different ways are possible. But they are not equivalent since the non-linearity of the model is activated differently. The first combination uses ATL and CLIM. The difference between these two experiments gives a direct evaluation of the impact exerted by the North Atlantic. The second combination uses GLOBAL and NOATL. It gives us not only the direct influence of the North Atlantic, but also the non-linear response through interaction with other oceanic basins.

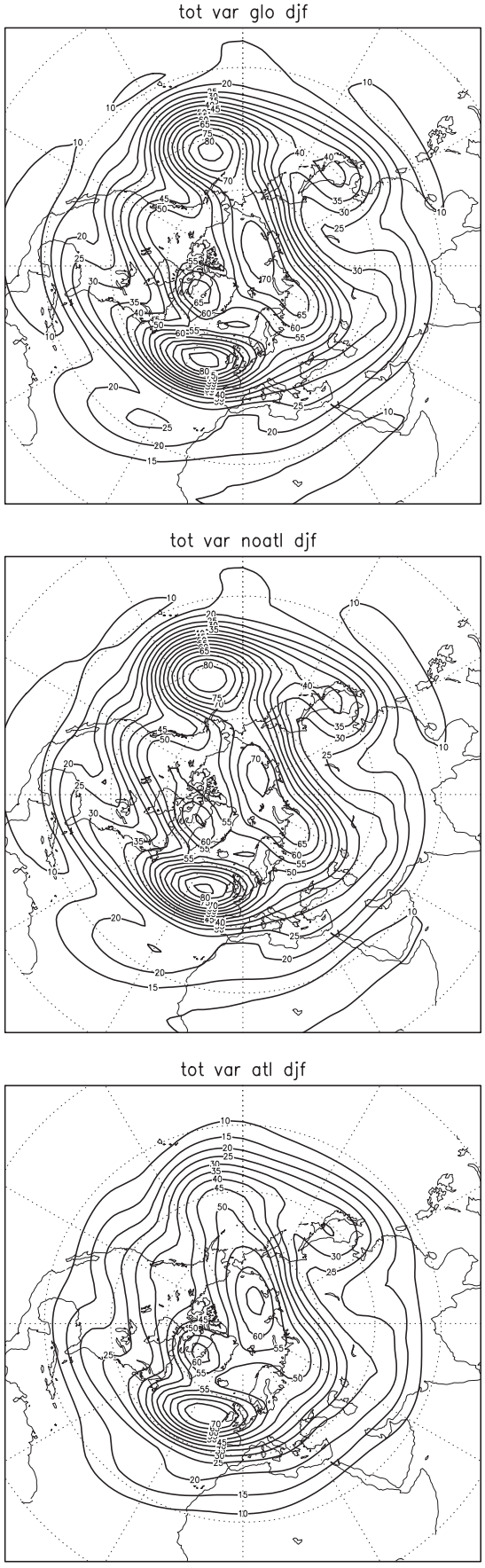

3.1. *Total variance*

The total variability (interannual standard deviation) of the geopotential height at 500 hPa simulated in GLOBAL, NOATL and ATL (fig. 1) can be compared with the estimation from the NCEP reanalysis (fig. 5b). While the simulated variability is overestimated in the high latitudes, it is, however, too weak at low latitudes. A local maximum over Greenland is present in the model as in the observations. But this maximum is too geographically confined for all three experiments, compared to the observed strong one. Furthermore, in the three experiments, a strong maximum is located just in the west of England over the North Atlantic. Two other local maxima in the north of the Siberian plain and in the north of Japan are well represented in the model. The center over the North Pacific, well identified in the observation, is also present in GLOBAL and NOATL, but not in ATL.

3.2. *Internal variance*

At first glance, the spatial structure, even the magnitude, of the internal variability (fig. 2) is very close in the three experiments. The resemblance to the CLIM is also evident (see fig. 5a). It is mainly zonally distributed, increasing from low to high latitudes. The maxima located over the North Atlantic, Greenland and Siberia are still present, but not the center over the North Pacific. The fact that different estimations of the internal variance give similar results indicates that the internal variance is a robust variable, almost intrinsic to the model's fundamental behaviour. However careful examination still reveals subtle differences among the experiments, which is the manifestation of the non-linearity and the interaction between the model's forced behaviour and its random variation. In

Fig. 1. Total variability (expressed as interannual standard deviation, in meters) for winter (December-January-February) 500-hPa geopotential height in respectively GLOBAL, NOATL and ATL experiments.

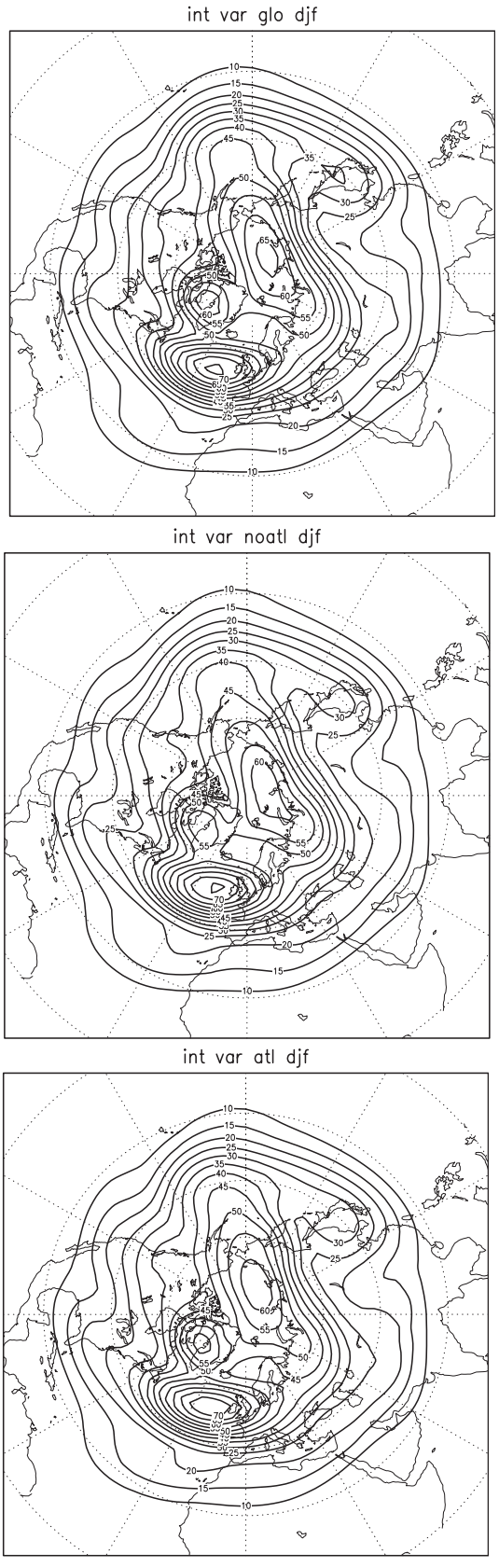

Fig. 2. Same as in fig. 1, but for the internal variability.

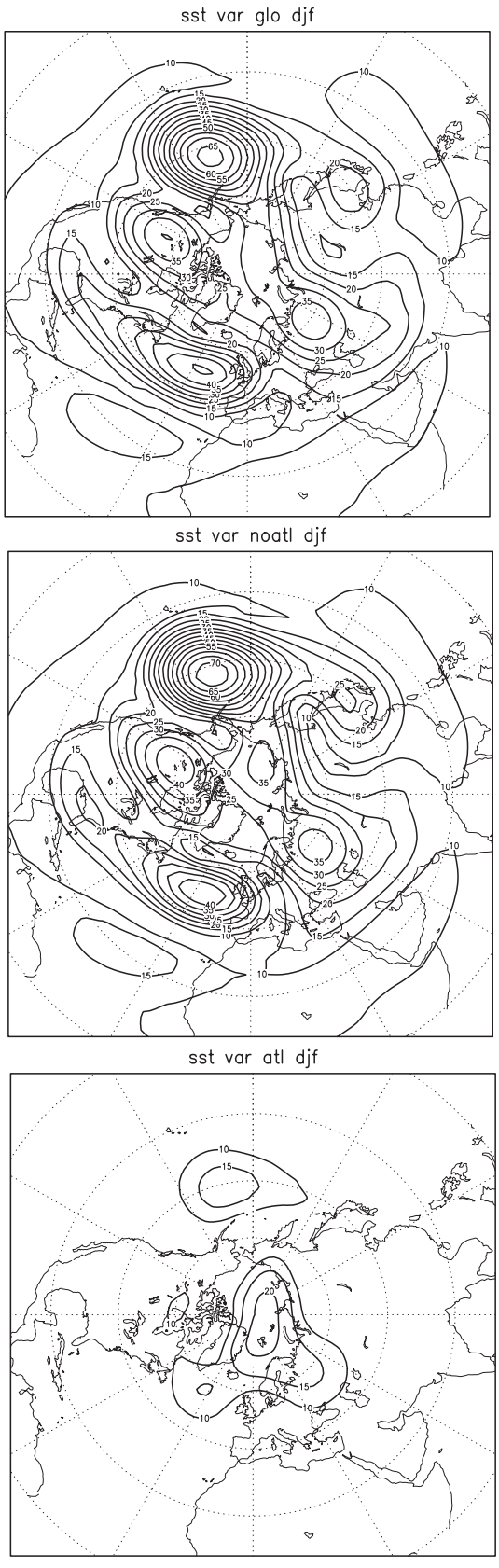

Fig. 3. Same as in fig. 1, but for the external forced variability.

fact, oceanic conditions are able to modulate the mean atmospheric circulation and also its transient properties.

3.3. *Forced variance*

The forced variability is displayed in fig. 3 for the three experiments. The forced variance deduced from ATL is a direct estimation of the impact exerted by the North Atlantic. It is in general very weak. But we can still observe high-value centers over the Arctic and North Pacific. These remote influences are probably due to the hemispheric teleconnection mechanism. The local influence over the North Atlantic is however small.

The structure of the forced variance has a good resemblance between GLOBAL and NOATL. Their difference gives another evaluation for the role played by the North Atlantic. Visual inspection shows that the forced variance decreases, from NOATL to GLOBAL, over the North Pacific and North America, but increases in the Atlantic sector. This is probably due to the interaction between the North Atlantic variability and that of other oceanic basins. The final forced variance can thus be increased or decreased for different geographical locations. A more precise interpretation of this modulation is presented later.

3.4. *Potential predictability*

The potential predictability (fig. 4) induced by the North Atlantic Ocean alone is very weak (< 10%). It is not significant in large parts of the Northern Hemisphere, except in a marginal region over the Eastern Pacific where the total variability is very weak and over the Arctic.

For the experiments GLOBAL and NOATL, the potential predictability (fig. 4) is also weak,

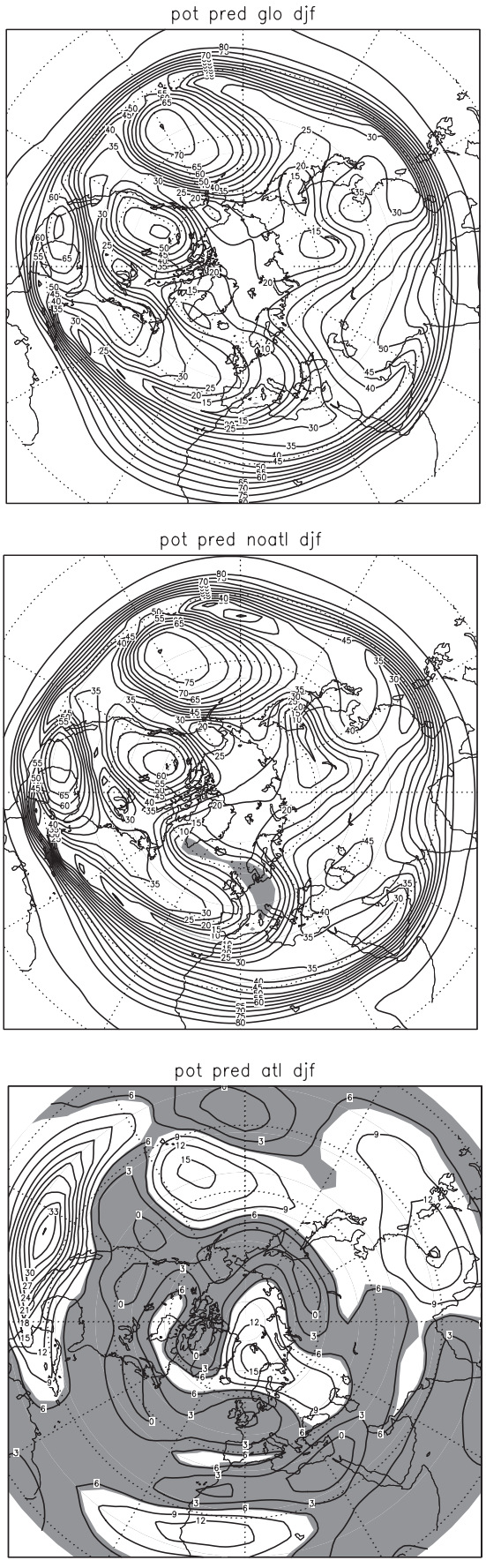

Fig. 4. Potential predictability (% of total variance) for winter (DJF) 500-hPa geopotential height in GLOBAL, NOATL and ATL. Shaded regions indicate non-significant zone according to an *F* test (see text).

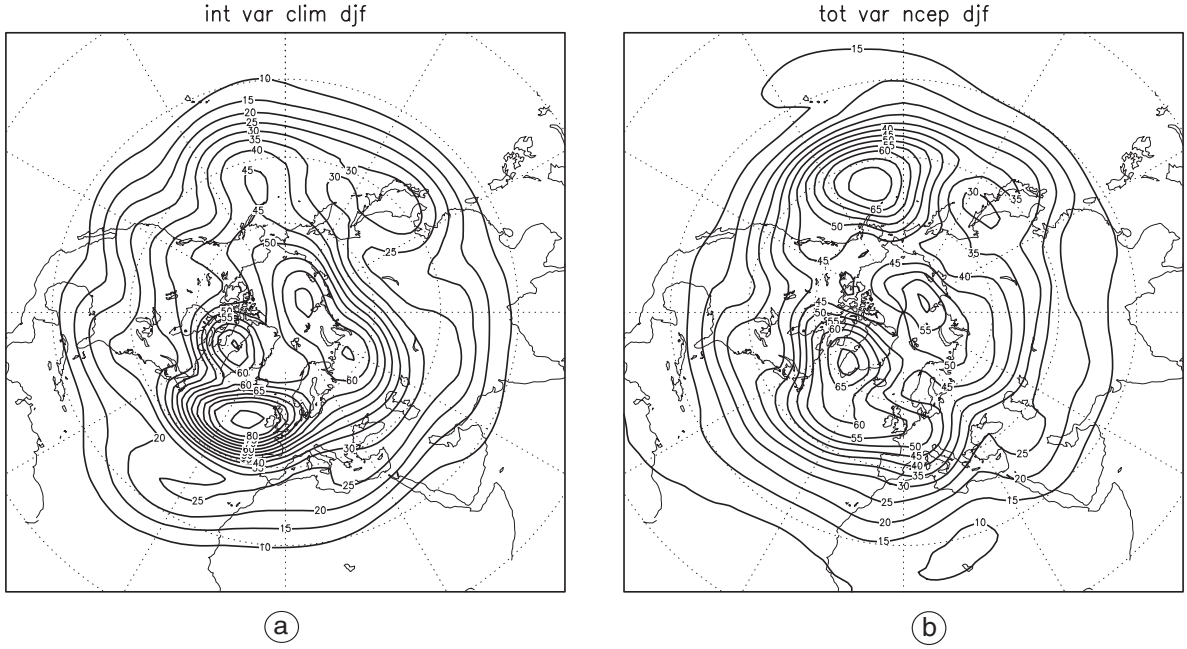

Fig. 5a,b. Interannual variability (in meters) for winter (DJF) 500-hPa geopotential height in the CLIM experiment (a) and in the NCEP reanalysis data set (b).

with values of 10% over Europe and 50% over the North Pacific, North America and the Gulf of Mexico. This seems coherent with results reported in Kumar and Hoerling (1998) and Cassou and Terray (2001).

The general feature for the potential predictability is its almost zonal distribution with, however, larger values over ocean than over land. In addition, at low latitudes the atmospheric internal variability is weaker and the potential predictability is higher.

We already know that the North Atlantic forcing can modify both internal and external variances through complex nonlinear interaction with other oceanic basins. Modifications in the internal and external variances lead finally to changes in the potential predictability. Over the North Pacific and North America, comparison between NOATL and GLOBAL reveals a weakening of the forced variability and an increase in the internal variability at the same time. The potential predictability over this region is thus largely reduced by incorporation of the North Atlantic. The inverse situation is found in the sector of the North Atlantic, *i.e.*, the potential predictability is improved by the incorporation

Table I. Regional-averaged values of the total, internal and forced variability for the three experiments ATL, NOATL and GLOBAL. The average is over the PNA (Pacific-North-America) region (145°E/80°W and 30/80°N). Last raw gives the values of potential predictability. The 99% (or 95%) significance level is reached when potential predictability is 6.4% (or 4.3%) for ATL and NOATL, and 6.2% (or 4.2%) for GLOBAL

Experiment	ATL	NOATL	GLOBAL
Total variability (m)	55.7	59.9	63
Internal variability (m)	54.8	50.3	55.4
External variability (m)	9.7	32.6	30.1
Pot. predictability (%)	2.4	29.4	22.7

Table II. Same as in table I, but for the region NAE (North-Atlantic-Europe) (80°W/20°E and 30/90°N).

Experiment	ATL	NOATL	GLOBAL
Total variability (m)	52.2	56.3	57.5
Internal variability (m)	50.6	51.9	52.5
External variability (m)	13	21.9	23.3
Pot. predictability (%)	6.6	15.2	16.3

of the North Atlantic oceanic information since the internal variability is reduced and the external one enhanced.

To summarize and quantify our results, we performed a regional average for these two particular regions. Tables I and II give respectively the total, internal and external variances, and the potential predictability for the PNA and NAE (North-Atlantic-Europe) regions. The three experiments ATL, NOATL and GLOBAL are all included. There is a slight general increase in the total variance from ATL to NOATL, then to GLOBAL. However, their decomposition into internal and external variances and their respective evolution make the final potential predictability very different. In the remote PNA region, the direct impact of the North Atlantic is weaker than over North Atlantic/Europe. However the non-linear estimation suggests that this direct influence is largely modified by its combination with other ocean forcings. Indeed, over the PNA region the potential predictability is substantially reduced by the presence of the North Atlantic forcing due to decreased external response and increased chaotic variability. In the NAE region the modulation of the potential predictability is weak. The external signal is stronger with the North Atlantic forcing but the internal variability is also increased.

4. Modal analysis

From the results presented above, we can notice some regional coherence in the vicinity of the well-known centers of action in the atmosphere. It is thus possible that the atmospheric response to the oceanic boundary forcing is modal and can be studied through the modification of its basic regimes and global teleconnection structures. We will then pursue our investigation, no longer in the physical domain, but rather in the «spectral» domain. The ANOVA technique will be used to analyze the time coefficients of the dominant modes.

A natural decomposition of the atmospheric variability is to use the Empirical Orthogonal Function (EOF). The calculation is done in the same manner as in Barnston and Livezey (1987) through a rotated EOF analysis for the Northern Hemisphere 500-hPa geopotential height. We first perform the analysis for each of the three experiments in a separate way. The obtained principal modes of variability are very close among the experiments and comparable to those deduced from observed data, but their relative importance in explaining the total variance is different. In order to have a common comparison base, we performed the EOF analysis for the super-ensemble containing all members of the three experiments, one after another. The NCEP reanalysis data were also added to this super-ensemble as an additional member. The super-ensemble thus contained 36 (= 17+9+9+1) members. In this way, we obtained common coherent spatial patterns $\boldsymbol{X}^k(s)$ (where k indicates the EOF rank), but different time series, $\alpha_i^k(t)$, associated with each member i of the super-ensemble. We studed only the first $K = 6$ EOFs which represent near 70% of the total variance of the super-ensemble. The physical field $x_i(t, s)$ for each member i (including the NCEP reanalysis data) was thus decomposed into two parts

$$x_i(t,s) = \sum_{k=1}^{K} \alpha_i^k(t) \boldsymbol{X}^k(s) \; . \qquad (4.1)$$

Our objective was not to extract the most skillful or most reproducible modes, as can be done with SVD (Singular-Value Decomposition) analysis applied simultaneously to the simulation and observation, but rather to show the influence of oceanic conditions on the natural atmospheric dominant modes. The combined EOF technique extracts thus the common dominant spatial patterns $\boldsymbol{X}^k$ of the super-ensemble. The time series $\alpha_i^k(t)$ indicates the temporal of the corresponding spatial structure $\boldsymbol{X}^k(s)$ for each simulation i (including the NCEP reanalysis data set). The projection (noted as $\boldsymbol{Y}_i^k$) of a particular member $x_i(t, s)$ on its own time series $\alpha_i^k(t)$ illustrates the manifestation of the common spatial structure $\boldsymbol{X}^k(s)$ on this particular member

$$\boldsymbol{Y}_i^k(s) = \frac{1}{T} \sum_{t=1}^{T} \alpha_i^k(t) \, x_i(t,s) \; . \qquad (4.2)$$

Figure 6a-f shows the common EOF $\boldsymbol{X}^k$, while fig. 7a-f presents the particular projection map $\boldsymbol{Y}^k$ for the NCEP reanalysis data set. We also

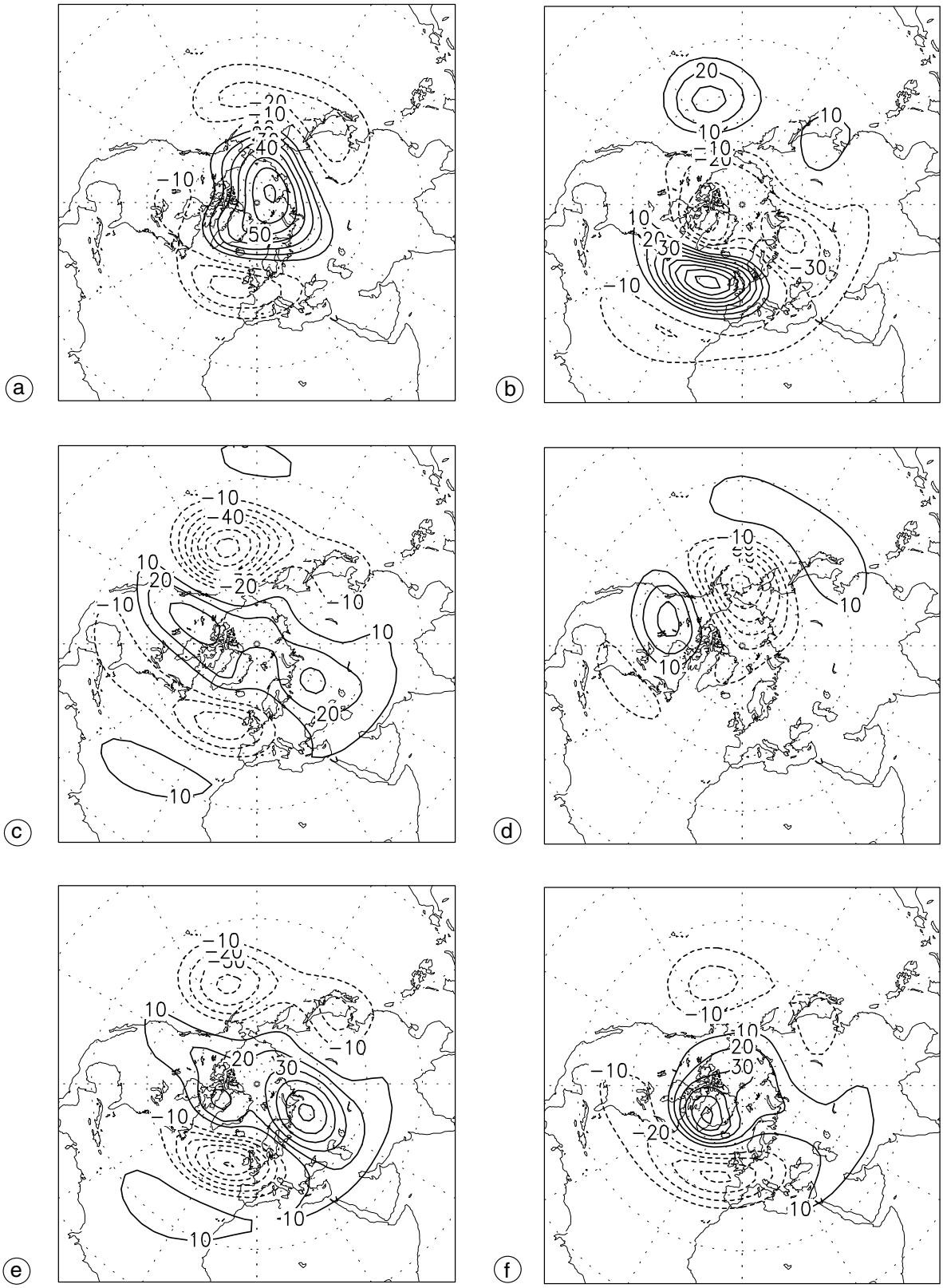

Fig. 6a-f. Common spatial structures obtained through the super-ensemble rotated EOF analysis for DJF-mean 500-hPa geopotential height in the Northern Hemisphere. The explained variance is respectively 16.2% (a); 13.4% (b); 12.3% (c); 10.7% (d); 9.5% (e), and 7.5% (f). Total variance is 302 m^2s^{-2}. Units are in meters.

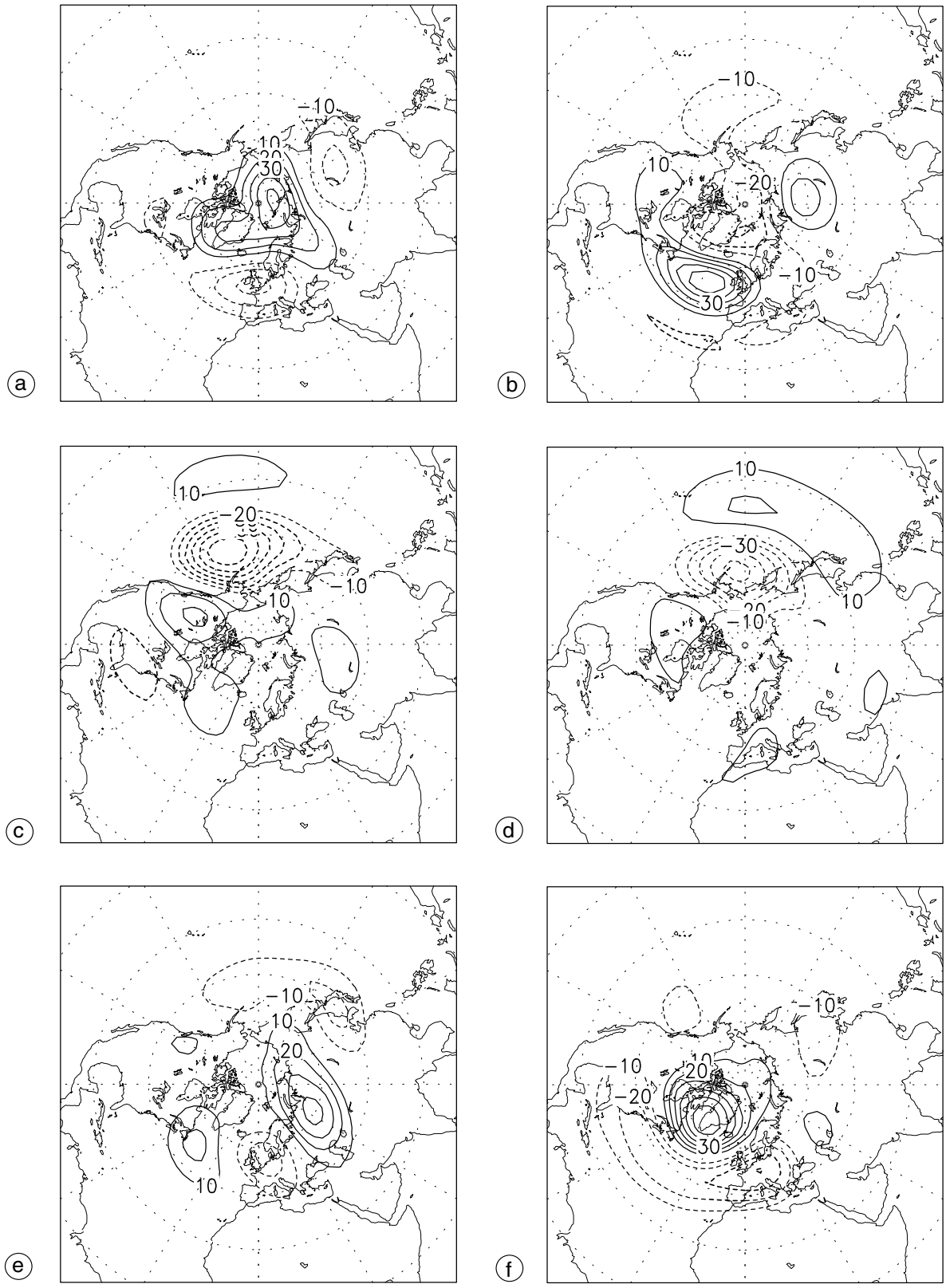

Fig. 7a-f. Projection of the common EOF structures (shown in fig. 6a-f) onto the NCEP reanalysis data set. Units are in meters.

performed EOF analysis separately for each member of the super-ensemble. The obtained spatial structures (not shown) are very similar to each other and close to the common structures in fig. 6a-f.

Figure 6a-f shows slight geographical displacements or distortion of the simulated structures compared to the observed ones (fig. 7a-f). Such discrepancies can be related to the systematic error of the background climatological flow (Kushnir *et al*., 2002). They are mainly due to the intrinsic atmospheric processes but they also mark responses to oceanic forcing (see Peng and Robinson, 2001). Except for some systematic errors, the model is, in general, able to simulate correctly the main observed global teleconnection structures (with spatial shifts, in many cases).

The dominant mode (accounting for 16.2% of the total variance) is the annular mode with a strong zonally symmetric pattern, looking like the AO pattern (Thompson and Wallace, 1998). The second mode (accounting for 13.4% of the total variance) has a strong center in the North Atlantic, near the European coast. This center is surrounded by a circle with opposite-sign values. A minor center with the same sign as in the North Atlantic can be observed in the North Pacific. This pattern (see fig. 7a-f) is similar to the observed East Atlantic pattern defined by Barnston and Livezey (1987). The third mode (12.2%) resembles to the well-known PNA pattern. The fourth mode (10.7%) has a strong wave-train pattern linking the North Pacific and North Atlantic through a cross-pole path. It corresponds to the observed West Pacific pattern. The fifth mode (9.5%) has a weak relation with the observed pattern. It is mainly present in the NOATL experiment and has a large regional difference in GLOBAL (no Pacific center) and is absent from ATL. The last mode that we considered accounts for 7.5% of the total variance. It is close to the observed NAO pattern (Hurrel and Van Loon, 1997).

Table III. Results from ANOVA technique (internal variance, external variance and potential predictability) for different dominant atmospheric modes and for the experiment ATL. The 99% significance level is reached when potential predictability is 6.34%.

Mode number	1	2	3	4	5	6
Internal variability (m)	110	98	65	92	76	77
External variability (m)	33	10	21	0	15	11
Pot. predictability (%)	8.2	1	9.6	0	4	1.8

Table IV. Same as in table III, but for the experiment NOATL. The 99% significance level is reached when potential predictability is 6.34%.

Mode number	1	2	3	4	5	6
Internal variability (m)	111	100	63	81	83	78
External variability (m)	54	56	104	57	56	28
Pot. predictability (%)	19.4	24.1	73.4	33.6	31	11.5

Table V. Same as in table III, but for the experiment GLOBAL. The 99% significance level is reached when potential predictability is 6.16%.

Mode number	1	2	3	4	5	6
Internal variability (m)	113	99	66	86	79	78
External variability (m)	56	61	94	59	59	31
Pot. predictability (%)	19.6	27.7	66.7	32.0	36.0	13.8

After this super-ensemble EOF analysis, we then applied the ANOVA technique to the reduced data sets, *i.e.*, the time coefficients $\alpha_i^k(t)$ for the first six dominant modes. Results are given in tables III, IV and V for the three experiments respectively. For the experiment ATL, potential predictability was weak for all the modes, since the oceanic forcing itself was very weak. However the first and third modes (annular mode and PNA pattern) reached almost 9%. For both the experiments NOATL and GLOBAL, the third mode has the largest potential predictability. However, the first mode (AO) and the sixth mode (NAO) have the smallest potential predictability.

The influence exerted by the North Atlantic Ocean can be assessed through the comparison between NOATL and GLOBAL. Further comparison with ATL can reveal the non-linear interaction with other oceanic basins. Let us take the first mode (AO), the experiment ATL shows that the incorporation of the North Atlantic oceanic variability leads to a potential predictability of 8.2%. For the NOATL and GLOBAL experiments, the potential predictability is almost

identical, showing no contribution of the North Atlantic oceanic variability. The non-linear effects through the interaction with other oceanic basins totally cancel the direct effect. This destruction effect is even stronger for the third mode (PNA) since we observe a significant decrease for the potential predictability from NOATL to GLOBAL. The inverse situation occured for modes 5 and 6 with an increase in the potential predictability from NOATL to GLOBAL, showing a positive contribution of the North Atlantic Ocean.

5. Summary and conclusions

By using an atmospheric general circulation model, we studied the atmospheric response to varying oceanic boundary conditions. The simulations cover the period from 1950 to 1994. Three ensemble simulations were performed with different configurations of the oceanic forcing to isolate the North Atlantic Ocean's role. We used a standard ANOVA technique to separate internal and external variability from total variability. The first ensemble GLOBAL was forced by the global observed oceanic surface conditions (SST and sea ice). The second ensemble NOATL was forced by the observed varying boundary conditions for the global ocean except for the North Atlantic where climatological conditions were used. The third experiment ATL is a complementary one with observed varying boundary conditions for the North Atlantic and climatological ones elsewhere.

Climate response to the North Atlantic forcing was first assessed through the ATL experiment. The direct forcing of the North Atlantic Ocean is weak. It mainly leads to a reduction of the internal variability and thus an increase in the potential predictability over the North Atlantic. The dominant annular mode is significantly affected by the North Atlantic forcing and is the major cause of this modification. The North Atlantic oceanic forcing creates a weak external signal in the North Pacific region but the internal variability also increases. The external variability is associated with the PNA pattern while the internal variability seems to be associated with the West Pacific pattern.

The role of the North Atlantic in conjunction with other basins is also assessed through the differences between the GLOBAL and NOATL experiments. The potential predictability over the North Atlantic sector is slightly enhanced. It is caused by the Eastern Atlantic pattern and the mode 5 but not by the AO pattern. Over the North Pacific and North America sector, internal variability is largely increased when the North Atlantic Ocean forcing is added. Moreover the external signal is significantly reduced and this leads to a decrease of the potential predictability. The reduced potential predictability is explained essentially by the modification of the PNA and WP modes. The variability created by the North Atlantic Ocean can be transmitted to the North Pacific region. Furthermore, it interacts with the Tropical Pacific forcing, leading to an increase in the random variability.

Our results suggest that the North Atlantic Ocean can influence the atmosphere in two different ways. It can drive an external signal which is potentially predictable but only weakly. It can also modify the internal variability. When those two modifications act together (reducing chaotic and increasing forced signal) the resulted potential predictability can become significant. But the influence of the North Atlantic is not linear. It interacts with forcings from other oceanic basins. This interaction can lead to a large modulation of the direct signal. In particular, over the North Pacific sector, the interaction of the direct North Atlantic signal with other oceanic responses (mostly from Equatorial Pacific) is destructive for the potential predictability, since it increases the chaotic fluctuations while it reduces the predictable forced response. So the inclusion of the North Atlantic forcing in conjunction with the Tropical Pacific reduces the potential predictability in the North Pacific. The potential predictability in the North Atlantic - Europe region is, however, slightly increased.

Acknowledgements

Computer resources were allocated by the IDRIS, the CNRS' computer center. This work is supported by the European Commission through the SINTEX project.

REFERENCES

BARNSTON, A.G. and R.E. LIVEZEY (1987): Classification, seasonality and persistence of low frequency atmospheric circulation patterns, *Mon. Weather. Rev*., **115**, 1083-1026.

CASSOU, C. and L. TERRAY (2001): Oceanic forcing of the wintertime low frequency atmospheric variability in the North Atlantic Europe sector: a study with the Arpege model, *J. Climate*, **14**, 4266-4291.

COLLINS, M. and M.R. ALLEN (2002): Assessing the relatives roles of initial and boundary conditions in interannual to decadal climate predictability, *J. Climate* , **15** (21), 3104-3109.

FELDSTEIN, S.B. (2000): The timescale, power spectra and climate noise properties of teleconnection patterns, *J. Climate*, **13**, 4430-4440.

FOUQUART, Y. and B. BONNEL (1980): Computations of solar heating of the earth's atmosphere: a new parametrization, *Beit. Phys. Atmos.*, **53**, 35-52.

FRAEDRICK, K. (1994): An ENSO impact on Europe? A review, *Tellus*, **46**A, 541-552.

FRANKIGNOUL, C. (1985): Sea surface temperature anomalies, planetary waves and air sea feedbacks in the middle latitudes, *Rev. Geophys*., **23**, 357-390.

HARZALLAH, A. and R. SADOURNY (1995): Internal *versus* SST forced atmospheric variability as simulated by an atmospheric general circulation model, *J. Climate*, **8**, 474-495.

HURREL, J.W. and H. VAN LOON (1997): Decadal variations in climate associated with the North Atlantic oscillation, *Climatic Change*, **36**, 301-326.

KUMAR, A. and M.P. HOERLING (1998): Annual cycle of the Pacific-North American seasonal predictability associated with different phases of ENSO, *J. Climate*, **11**, 3295-3309.

KUSHNIR, Y., W.A. ROBINSON, I. BLADÈ, N.M.J. HALLA, S. PENG and R. SUTTON (2002): Atmospheric GCM response to extratropical SST anomalies: synthesis and evaluation, *J. Climate*, **15** (16), 2233-2256.

LATIF, M., K. ARPE and E. ROECKNER (2000): Oceanic control of decadal North Atlantic Sea level pressure variability in winter, *Geophys. Res. Lett*., **27**, 727-730.

LE TREUT, H. and Z.X. LI (1991): Sensitivity of an atmospheric general circulation model to prescribed SST changes: feedback effects associated with the simulation if cloud properties, *Climate Dynamics*, **5**, 175-187.

LI, Z.X. (1999): Ensemble atmospheric GCM simulation of climate interannual variability from 1979 to 1994, *J. Climate*, **12**, 986-1001.

LI, Z.X. and S. CONIL (2003): A 1000-year simulation with the IPSL ocean-atmosphere coupled model, *Ann. Geophysics*, **46** (1), 39-46 (this volume).

LORENZ, E.N. (1975): Climate predictability: the physical basis of climate modelling, *WMO GRP Pub. Ser.* 16, 132-136.

MEHTA, V.M., M.J. SUAREZ, J.V. MANGANELLO and T.L. DELWORTH (2000): Oceanic influence on the North Atlantic Oscillation and associated Northern Hemisphere climate variations, *Geophys. Res. Lett*., **27**, 121-124.

MORCRETTE, J.J. (1991): Radiation and cloud radiative properties in the ECMWF operational weather forecast model, *J. Geophys. Res.*, **96**D, 9121-9132.

PENG, S. and W.A. ROBINSON (2001): Relationships between atmospheric internal variability and the responses to an extratropical SST, *J. Climate*, **14**, 2943-2959.

RAYNER, N.A., E.B. HORTON, D.E. PARKER, C.K. FOLLAND and R.B. HACKETT (1996): Version 2.2 of the global sea ice and sea surface temperature data set, *Climate Research Technical Notes of the Hadley Center, 74.*

RODWELL, M.J., D.P. ROWELL and C.K. FOLLAND (1999): Oceanic forcing of the wintertime North Atlantic oscillation and European climate, *Nature*, **398**, 320-323.

ROWELL, D.P. (1998): Assessing potential seasonal predictability with an ensemble of multidecadal GCM simulations, *J. Climate*, **11**, 109-120.

SADOURNY, R. (1975): The dynamics of finite difference models of the shallow water equations, *J. Atmos. Sci.*, **32**, 680-689.

SADOURNY, R. and K. LAVAL (1984): January and July performance of the LMD General Circulation Model, in *New Perspectives in Climate Modelling*, edited by A. BERGER and C. NICOLIS (Elsevier Science Publishers, Amsterdam), 173-198.

SCHEFFE, H. (1959): *Analysis of Variance* (John Wiley and Sons), pp. 477.

THOMPSON, D.W.J. and J.M. WALLACE (1998): The arctic oscillation signature in the wintertime geopotential height and temperature fields, *Geophys. Res. Lett*., **25**, 1297-1300.

TIEDKE, M. (1989): A comprehensive mass flux scheme for *cumulus* parametrization in large scale models, *Mon. Weather Rev*., **117**, 1779-1800.

TRENBERTH, K.E., G.W. BRANSTATOR, D. KAROLY, A. KUMAR, N.C. LAU and C. ROPELEWSKI (1998): Progress during TOGA in understanding and modelling global teleconnections associated with tropical sea surface temperatures, *J. Geophys. Res*., **103**, 14,291-14,324.

VENZKE, S., M.R. ALLEN, R.T. SUTTON and D.P. ROWELL (1999): The atmospheric response over the North Atlantic to decadal changes in sea surface temperatures, *J. Climate*, **12**, 2562-2584.

VON STORCH, H. and F. W. ZWIERS (1999): *Statistical Analysis in Climate Research* (Cambridge University Press), 173-180.

WALLACE, J.M. and D.S. GUTZLER (1981): Teleconnections in the geopotential height field during the Northern Hemisphere winter, *Mon. Weather Rev*., **109**, 784-812.

ZWIERS, F.W., X.L. WANG and J. SHENG (2000): Effects of specifying bottom boundary conditions in an ensemble of atmospheric GCM simulations, *J. Geophys. Res*., **105**, 7295-7315.